Hemoglobin becomes electroactive upon interaction with surface-protected Au Nanoparticles.

*Rafael del Caño,[1] Lucia Mateus,[1,2] Guadalupe Sánchez-Obrero,[1] José Manuel Sevilla,[1] Rafael Madueño,[1] Manuel Blázquez,[1] Teresa Pineda[1]**

[1] Department of Physical Chemistry and Applied Thermodynamics. Institute of Fine Chemistry and Nanochemistry. University of Cordoba, Campus Rabanales, Ed. Marie Curie 2ª Planta, E-14014 Córdoba, Spain

[2] Present address: Corporación Tecnológica de Bogotá, Bogotá, Colombia.

AUTHOR EMAIL ADDRESS tpineda@uco.es

Abstract

In this work, we report on the electrochemical behavior of bioconjugates prepared with gold nanoparticles (AuNP) capped with three different molecular layers (citrate anions, 6-mercaptopurine and ω-mercaptoundecanoic acid) and the protein hemoglobin (Hb). Freshly formed bioconjugates are deposited on a glassy carbon electrode and assayed for electroactivity. A pair of redox peaks with formal potential at -0.37 V is obtained, in contrast with the free Hb protein that is inactive on the glassy carbon substrate. The redox response is typical for quasi-reversible processes allowing the determination of the electron transfer rate constant for the three bioconjugates. Additional evidence of the structural integrity of protein upon forming the bioconjugate is obtained by monitoring the electrochemical response of the Hb heme Fe(III)/Fe(II) redox couple as a function of solution pH. Moreover, the Hb forming the protein corona around the AuNPs show good electrocatalytic activity for the reduction of hydrogen peroxide and oxygen. It has been found that only the first layer of Hb surrounding the AuNPs are electroactive, although some part of the second layer also contribute, pointing to the role of the AuNP in the electrochemical response.

Keywords: hemoglobin, gold nanoparticles, protein corona, electron transfer, electroactivity.

Introduction

Direct electrochemistry of redox proteins is difficult to realize in the normal working electrodes due the deeply burying of the electroactive centers or the unfavorable orientation of the proteins upon adsorption on the electrode surface. To accelerate the electron transfer rate, different chemically modified electrodes have been used that can shorten the distance between the active centers and the electrodes by directing the protein to immobilize in the right orientation [1-3]. In this sense, nanostructured materials and nanomaterials of various nature and morphologies are now being used for electrode modification taking advantage of their high conductivity, large surface area and good biocompatibility, to facilitate electron transfer of redox proteins [1]. The challenge is to develop an appropriate system for immobilization of the redox protein in a way that the electron transfer rate increase with respect to the classical metallic substrates.

Hemoglobin (Hb) is a typical metalloprotein with a quaternary structure that contains four polypeptide chains (globin chains) and one heme group bound to each of the globin chains. However, as an intrinsic protein [4, 5], Hb do not has a redox protein as natural partner for ET exchange and therefore it may lack of electron tunneling pathways within their own structure. This should be the reason of an inefficient ET when Hb is studied by using a naked electrode. Even though, Hb direct electrochemistry has been realized on different modified electrodes by using biopolymers [6, 7], membranes [8] and nanocomposites [9, 10].

Protein-nanoparticle conjugates, in particular those formed with gold nanoparticles (AuNPs), are widely used for different applications [11]. The good biocompatibility of AuNPs [12] together with the easy modification chemistry [13-15], the unique size-dependent chemical, physical and optical properties and high protein loading, make them very good candidates to probe the ability to facilitate electron transfer of the protein Hb [16].

It is well known that protein adsorption readily takes place when the AuNPs contact the biological milieu provoking that the protein surface is surrounded by a corona of proteins [17-19]. The protein corona has a dynamic character and its evolution plays an important role in the interaction of the AuNPs with biological systems. Thus, it is of great interest for any biological application to understand how the process of protein adsorption and exchanges occurs and, more importantly, the integrity of these proteins upon taking part in the corona [20, 21].

In the present work, we carried out an electrochemical characterization of the bioconjugates formed upon mixing Hb with AuNPs protected by three different layers, either citrate anions (c-) or 6-mercaptopurine (MP) or ω-mercaptoundecanoic acid (MUA). We are interested in evaluating the functionality of the protein by examining the redox response of the bioconjugates deposited on a glassy

carbon electrode as well as studying the electrocatalytical properties of the Hb against hydrogen peroxide and oxygen.

Experimental Section

Reactants.

Hemoglobin, from bovine blood (Hb), 6-mercaptopurine (MP), ω-mercaptoundecanoic acid (MUA), and semiconductor grade purity sodium hydroxide were purchased from Sigma-Aldrich. Hydrogen tetrachloroaurate trihydrate (from 99.99% pure gold) was prepared using a literature procedure [22] and stored in a freezer at −20 °C. The rest of the reactants were from Merck analytical grade. All solutions were prepared with deionized water produced by Millipore system.

Synthesis of cAuNPs.

The synthesis of cAuNPs has been carried out by following a classic method [23] consisting of the reduction of $HAuCl_4$ by citrate anions in an aqueous medium to obtain an average diameter of 13 nm. The synthesis of MP-AuNPs and MUA-AuNPs has been carried out by adding a 10-fold excess of either MP or MUA to a cAuNPs alkaline aqueous solution. Under these experimental conditions, only a slight change in the localized surface plasmon resonance (LSPR) band of around 3 nm after the modification was observed. The samples of MP- and MUA-AuNPs were dialyzed against a 10 mM NaOH solution to remove the reactant molecules that had not reacted with the AuNPs. The formation of the self-assembled monolayer concomitant to the displacement of citrate ions from the AuNP surface has been demonstrated by FT-IR spectroscopy [13, 15].

Formation of Bioconjugates.

The bioconjugates were formed by adding the appropriate amounts of AuNPs to Hb protein solutions a pH 7.4 [16]. The solutions of bioconjugates could interact for 30 min before the electrochemical measurements.

Characterization Techniques.

TEM images were obtained with a JEOL JEM 1400 instrument operating at 80-120 kV and analyzed using Image Pro Plus software (Servicio Apoyo a la Investigacion (SCAI) Universidad de Cordoba). Samples were prepared by casting and evaporating a droplet of nanomaterial solutions onto Formvar-coated Cu grids (400 mesh, Electron Microspopy Sciences). The micrographs obtained for either cAuNPs or Hb-cAuNPs are shown in Figure 1. It can be observed that whereas the cAuNPs aggregate in some extension, the bioconjugates are well separated probably due to the presence of the protein film that form the corona.

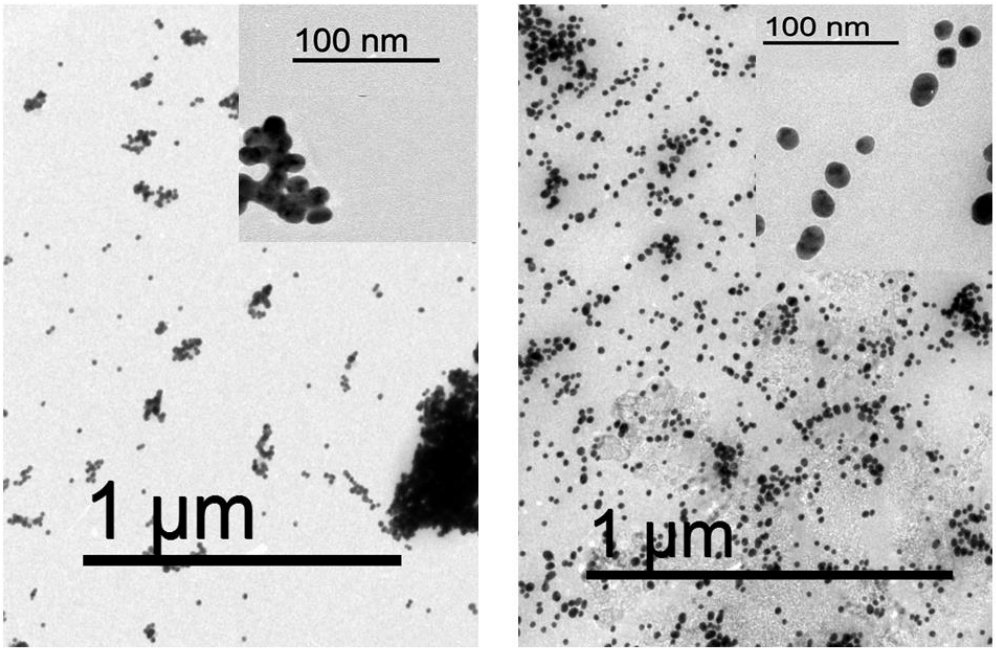

Figure 1. TEM micrographs of cAuNPs (left) and Hb-cAuNPs (right) at two different resolution.

Electrochemical experiments were performed using an Autolab (Ecochemie model Pgstat20) instrument attached to a PC with proper software (GPES and FRA) for the total control of the experiments and data acquisition. A conventional three electrode cell comprising a platinum coil as the counter electrode, a saturated calomel electrode as the reference electrode and a glassy carbon (GC) as the working electrode were used. Before each electrochemical measurement, the electrode was polished by using alumina slurries and sonicated in an ultrasound bath. After that, the clean electrode was cycled in a potential range from -1.1 to +1.1 V in 50 mM phosphate buffer at pH 7.4 up to a reproducible profile typical of a clean GC electrode was obtained. This surface treatment was the most appropriate to produce a surface that is clean, ordered and highly reproducible.

Results and Discussion

Direct electrochemistry of Hb bound to AuNPs.

In a recent publication, we have demonstrated that the protein Hb form stable bioconjugates with AuNPs capped with different molecular layers and that the protein structure is kept under conditions of colloidal stability [16]. To check that the electrochemical properties of the Hb protein are influenced by the interaction with the AuNPs, recently formed bioconjugates were deposited on the surface of a glassy carbon electrode and, after drying in a N_2 atmosphere, the electrochemical response, in the potential range of heme electron-transfer was registered (Scheme 1). We add the bioconjugates already formed, to emphasize the role of the protein corona in the electrochemical properties of the protein as most of the

studies reported up to now deal with protein supported on an array of AuNPs or other nanomaterials. In contrast to what it is observed with the free protein under similar experimental conditions, the bioconjugates show an electrochemical reversible response (Figure 1). The bioconjugate Hb-cAuNPs exhibits a couple of well-defined peaks at -0.351 and -0.389 V vs. SCE which could be ascribed to the direct electron transfer between Hb and the underlying GCE electrode surface, mediated by the cAuNPs. The formal potential $E^{o'}$ was -0.37 V in agreement with previous studies on the direct electrochemistry of Hb by using AuNPs mixed with MWCNTs [24], silk fibroin [25], carbon paste electrode [9], core-shell structurally Fe_3O_4 [26], cationic polyelectrolyte [27], flower-like zinc oxide/graphene composite [28], quaternized cellulose in a film composed of poly(ethylene glycol diglycidil ether) [29], carbon aerogel [30], layer-by-layer assembly with chitosan and graphene [31], within others.

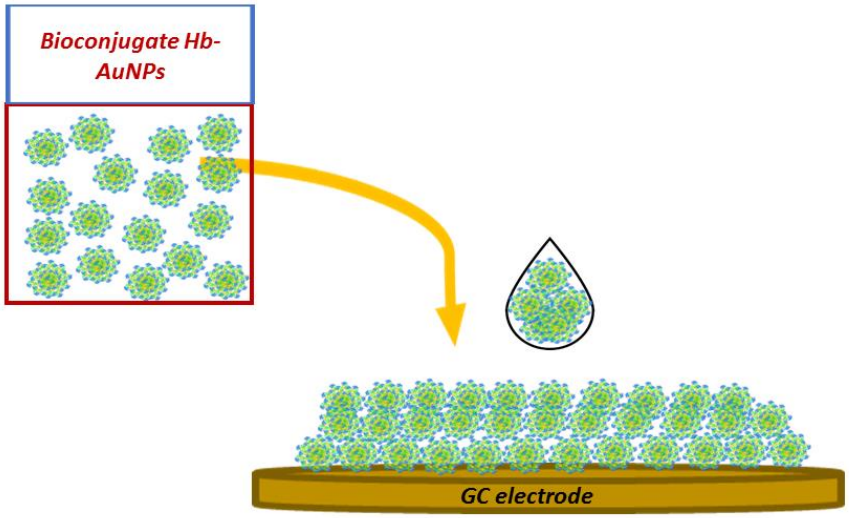

Scheme 1. Bioconjugates Hb-AuNPs dropped in a GC electrode.

The high solubility of the Hb-AuNP bioconjugates provokes that, once they are in contact with the electrolyte solution, tend to solubilize and the electrochemical response disappears in the successive potential cycles. To avoid this, after the deposited amount of the bioconjugate is dried, a thin film of nafion (0.1 % Nafion ethanolic solution) is applied on top to keep the material adsorbed in the electrode surface. Under these conditions the electrochemical signal is maintained after hours of continuous cycling (Figure 2a).

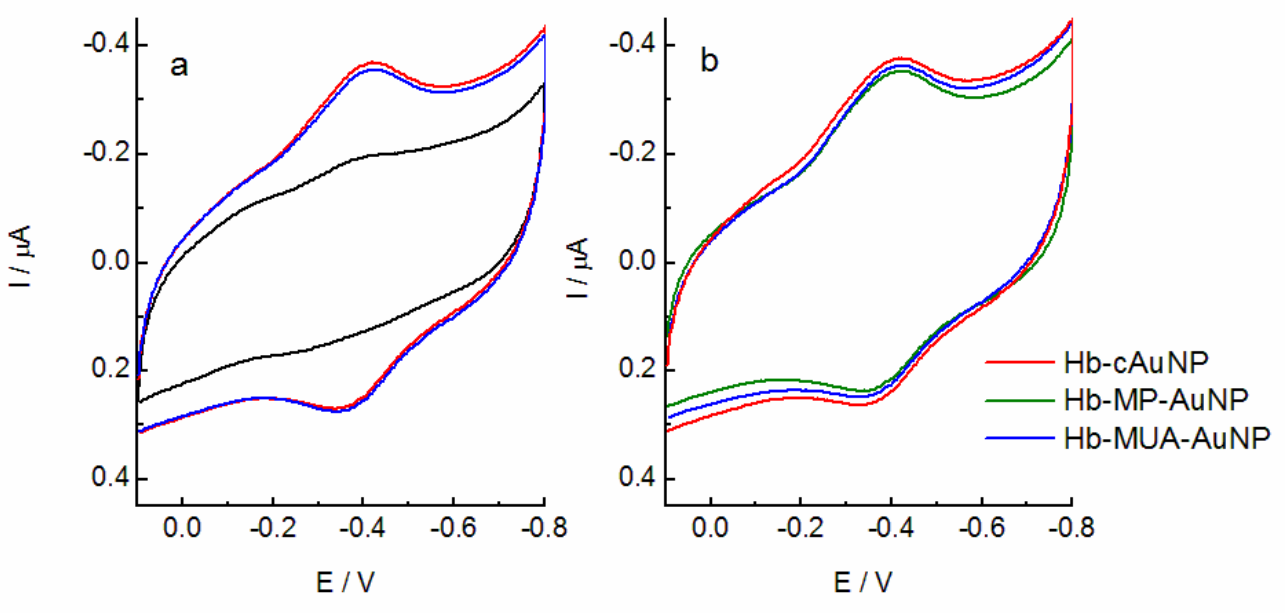

Figure 1. (a) Cyclic voltammograms of Hb (black) and Hb-cAuNPs deposited on a glassy carbon electrode in 50 mM phosphate buffer at pH 7.4. Curve red was obtained upon electrode immersion in the buffer solution and curve blue was obtained after 1 h of continuous cycling. (b) Cyclic voltammograms of the bioconjugates recorded under the same experimental conditions as in (a).

It is interesting to note that the peak potential separation (ΔEp) is 38 mV (at 0.1 V/s), indicating that the AuNPs facilitate the electron transfer of the Hb(Fe(III/II)) redox couple. For the three bioconjugates formed from c-, MUA- and MP-AuNPs (Figure 2b), the separation between the anodic and cathodic potentials are around 30 to 40 mV at the scan rate of 0.1 V/s, again as it is typical for an electron transfer process that is fast and quasi-reversible.

The influence of the scan rate on the electrochemical responses of these electrodes was investigated and the results are shown in Figure 3 for the bioconjugate Hb-cAuNPs. A pair of well-defined quasi-reversible peaks are observed in the cyclic voltammograms with almost equal height of the redox peak currents. Moreover, the anodic and cathodic current intensities vary linearly with the scan rate from 0.02 to 0.8 V/s, and this dependence in the logarithmic scale (Figure 3, inserts) is close to unity indicating that the process is surface controlled as expected since the bioconjugates are entrapped under the nafion film. The shapes of the cyclic voltammograms are also typical for redox processes in the adsorbed state. Thus, the peak current in the redox process are represented by eqn 1 [32, 33].

$$i_p = \frac{n^2 \cdot F^2}{4RT} \cdot v \cdot A \cdot \Gamma = \frac{n \cdot F \cdot Q \cdot v}{4RT} \qquad (1)$$

where i_p are the anodic or cathodic current, n is the number of electrons transferred, F is the Faraday constant, v is the scan rate, A is the electrode area, Γ is the surface coverage and Q is the charge involved in the electrochemical process, calculated by integration of the voltammogram after background

subtraction. The integration of the reduction and oxidation peaks gave nearly constant charge with different scan rates, result that is typical for a thin layer electrochemical behavior [34]. From the slope of the Ip vs. v curve, n was calculated to be about 0.8, meaning that one electron is involved in the redox reaction.

Surface coverages obtained by applying eqn 1 are gathered in Table 1. To determine the surface coverage, we have used the total surface area of the AuNPs contained in the bioconjugates. Taking advantage of the fact that the electrochemical signal is only produced by the Hb protein added in the form of bioconjugate as no response is obtained in the absence of AuNPs (see Figure 1), we can ascribe the electrochemical signal to the Hb units belonging to the bioconjugate. As the amount of bioconjugate entrapped under the film is known, and the size of the AuNP is well defined, the gold surface area is readily determined (0.0149 cm^2, in the present experiments). In Table 1, the number of Hb molecules per AuNP giving the electrochemical signal are also included.

In a roughly calculation, using the Hb dimensions reported of 6.5 x 5.5 x 5.0 nm [35], the surface area occupied by a Hb tetrameric unit assuming a molecule with the long axis parallel to the metal surface is 32-35 nm^2. Under these conditions, the theoretical monolayer surface coverage is of 1.89 x 10^{-11} mol/cm^2 (for protein monomers) and then, the experimental values correspond to approximately 7, 6 and 7 monolayers of protein for c-, MP- and MUA-AuNPs, respectively. However, by considering the nanoparticle spherical shape and the influence of increasing the radio in the number of molecules that can accommodate in the successive layers [36], we can determine that the number of Hb needed to form the compact layers around the AuNP are 15, 65 and 150 for the first, second and third corona layers, respectively (Scheme 2). Therefore, the results obtained indicate that the first protein layer is always involved in the electron exchange but, only a portion of the second layer can participate in the electron transfer process.

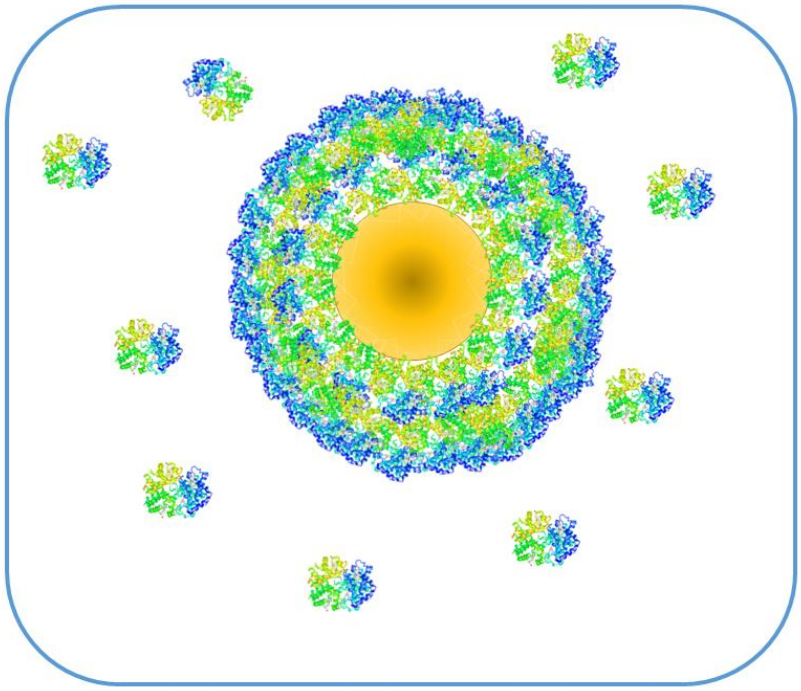

Scheme 2. The number of protein on the corona layers depends on the actual bioconjugate radio.

Table 1. Surface coverages (determined as mol of electron per cm^2), number of Hb molecules (as tetramers) per bioconjugate unit and electron transfer rate constants of the bioconjugates.

Bioconjugate	Γ / $mol \cdot cm^{-2}$	Hb / AuNP	k_s / s^{-1}
Hb-cAuNP	1.39×10^{-10}	28	1.29
Hb-MP-AuNP	1.23×10^{-10}	25	2.24
Hb-MUA-AuNP	1.30×10^{-10}	26	2.17

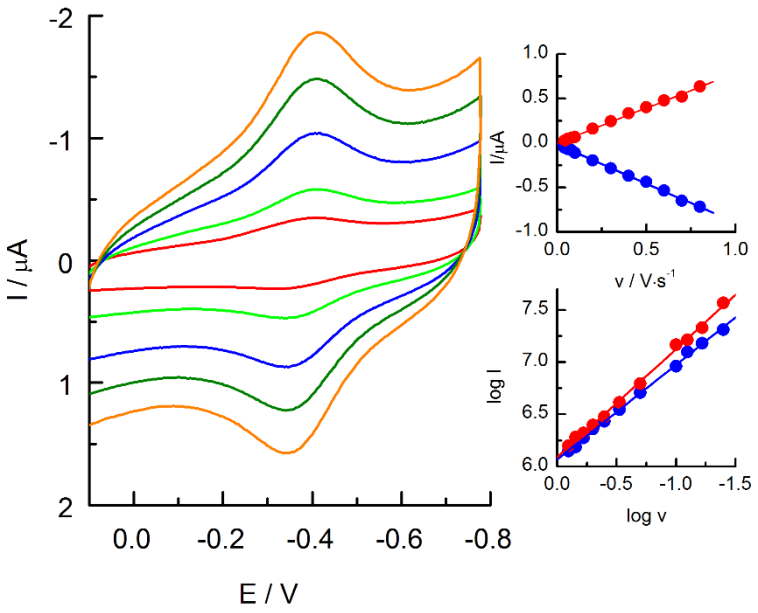

Figure 3. Cyclic voltammograms of Hb-cAuNPs deposited on a glassy carbon electrode as a function of scan rate in 50 mM phosphate buffer at pH 7.4. Insert: upper: plot of the current intensity vs scan rate; lower: logarithmic plot of the current intensity vs scan rate.

According to Laviron's model, when the anodic and cathodic peak potentials are linearly dependent on the logarithm of scan rates and ΔEp > 200/n mV, the electron transfer rate constant (k_s) can be determined by using eqns (2) and (3):

$$E_{pa} = E^{o'} + \frac{2.303RT}{(1-\alpha)nF}\left(\frac{log(1-\alpha)nF}{RT-logk_s}\right) + \frac{2.303RT}{(1-\alpha)nFlogv} \quad (2)$$

$$\Delta E_p = \frac{2.303RT}{(1-\alpha)\alpha nF}\left[\frac{\alpha \cdot log(1-\alpha)+(1-\alpha)\cdot log\alpha - logRT}{nF-logk_s}\right] + \frac{2.303RT}{(1-\alpha)\alpha \cdot n \cdot F \cdot logv} \quad (3)$$

The values obtained for the bioconjugates are also gathered in Table 1. These values are similar to those reported for AuNPs mixed with carbon aerogel [30], core-shell Fe_3O_4 nanostructured materials [26], gold nanorods modified with silica [37], and AuNPs modified gold electrode [38].

Effect of pH on the direct electrochemistry of the bioconjugates

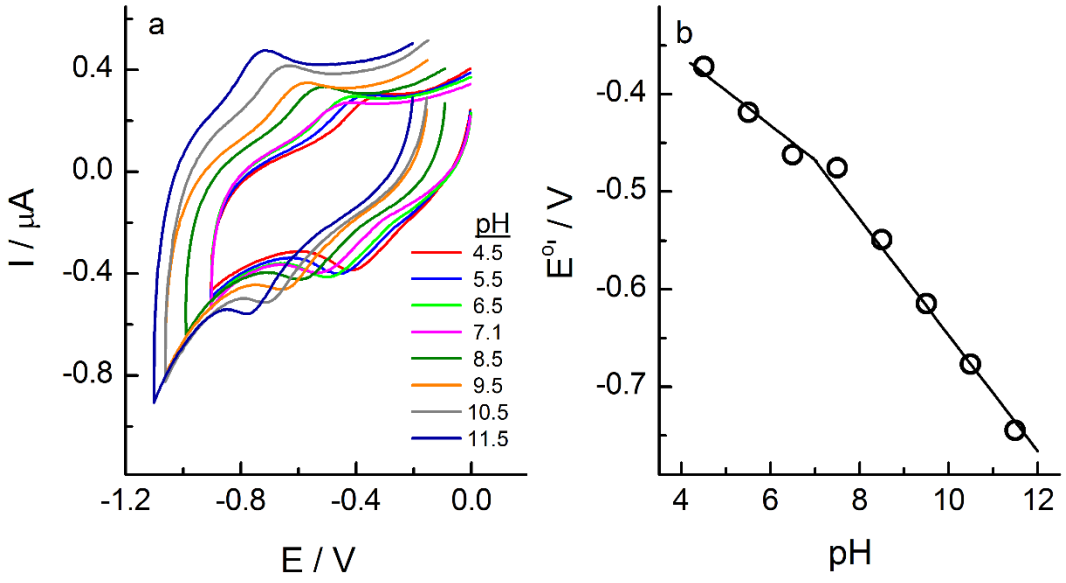

Figure 4. (a) Cyclic voltammograms of Hb-cAuNPs deposited on a glassy carbon electrode in 50 mM phosphate buffer as a function of pH. (b) Variation of the formal potential E°' as a function of pH.

The effect of the solution pH on the electrochemical behavior of the Hb-AuNP bioconjugates has also been explored. Figure 4a displays the cyclic voltammograms of the Hb-cAuNPs at different solution pH. The shapes of the redox peaks are maintained in all the pH values studied and the peak current slowly increases with pH. The anodic and cathodic peak potentials shifted negatively and hence the formal redox potential, E°' (Figure 4b), revealing that the redox process of Hb(Fe(III)/(II)) involved proton transfer. However, the observed trend can be fitted to two different lines that show a break at around pH 7. At pH > 7, the slope value is of 59 mV/pH, the theoretical value of the Nernst equation for a one proton couple single electron transfer reaction [39]. At pH < 7, the slope decreases up to a value of 35 mV/pH. This smaller value under acidic conditions, can be ascribed to a higher complexity of the process that must be influenced by the protonation of the amino acids and the water molecules, mainly in the heme environment [8]. The reaction involved in all the pH range can be represented as:

Hb heme(Fe(III)) + H^+ + e^- ↔ Hb heme(Fe(II))

The nature of the amino acid residues that are participating in the electrochemical process is unknown but, a role of the Histidine residue situated in the heme close environment cannot be discarded as the protonation state of these residues are closely connected with the interaction of the iron ion with the porphyrin ring in the different oxidation states and, therefore they have an apparent dissociation constant depending on the nature of these interactions.

Bioelectrocatalysis

There are many reports dealing with studies of proteins and enzymes containing the heme group, such as horseradish peroxidase, cytochrome c, Hb and myoglobin, demonstrating the ability of these proteins to reduce H_2O_2 and O_2 electrocatalytically [40-44].

The electrocatalytic activity of Hb-AuNPs bioconjugates towards the reduction of H_2O_2 has been investigated. As shown in Figure 5, with the addition of H_2O_2 into the phosphate buffer at pH 7.4, the reduction peak currents increased gradually, while the oxidation peak currents decreased and finally disappeared. This behavior is typical of these electrocatalytic systems where the generated Hb in the reduced state is immediately oxidized by H_2O_2 [45].

The cathodic current varies linearly with the H_2O_2 concentration in the range of 5 µM to 400 µM. The sensitivity of the Hb-AuNP bioconjugate electrodes are gathered in Table 2, together with the values of the other systems studied in the present work.

With the increase of H_2O_2 concentration, a response plateau which is characteristic of Michaelis-Menten behavior is observed. From these data an apparent Michaelis-Menten constant (K_M^{app}) can be calculated by using Lineweaver-Burk equation [45]:

$$\frac{1}{I_{SS}} = \frac{1}{I_{max}} + \frac{K_M^{app}}{I_{max}} \cdot \frac{1}{c} \qquad (4)$$

where I_{ss} is the steady-state current after the addition of substrate, c is the bulk concentration of the substrate, and I_{max} is the maximum current measured under saturated substrate conditions. The K_M^{app} can be obtained by analysis of the slope and intercept of the line by plotting the reciprocals of the steady-state current against H_2O_2 concentration. The values obtained are also gathered in Table 2 and they are somewhat higher than those obtained with other system as layer-by-layer Hb/chitosan/graphene (0.66 mM) [31], but lower than that for Hb/Au/SBA15/GCE (2.87 mM) [46].

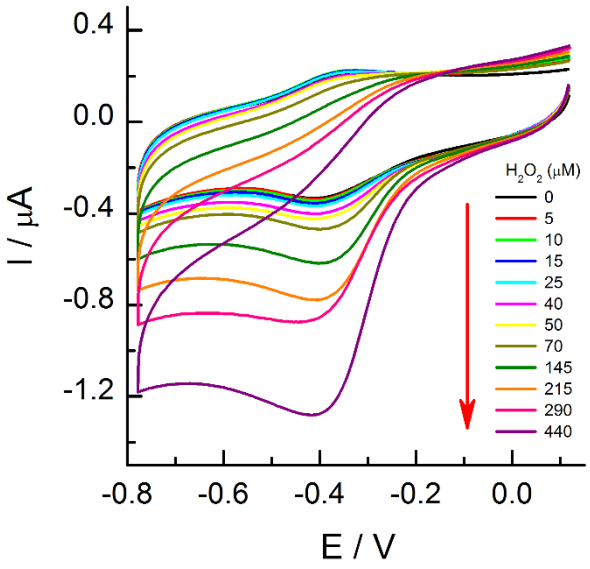

Figure 5. Effect of the addition of increasing concentrations of H_2O_2 to a 50 mM phosphate buffer solution at pH 7.4 with Hb-cAuNPs deposited on a glassy carbon electrode.

Table 2. Electrocatalytic parameters determined for H_2O_2 with the bioconjugates deposited on a GC electrode.

Bioconjugate	I_{max} / µA	K_M / mM	S / µA·mM^{-1}
Hb-cAuNP	2.0	1.2	2.1
Hb-MP-AuNP	3.0	1.4	2.1
Hb-MUA-AuNP	4.1	1.9	1.8

The small K_M^{app} implies a good affinity between the immobilized Hb and H_2O_2, favoring the electrochemical reaction.

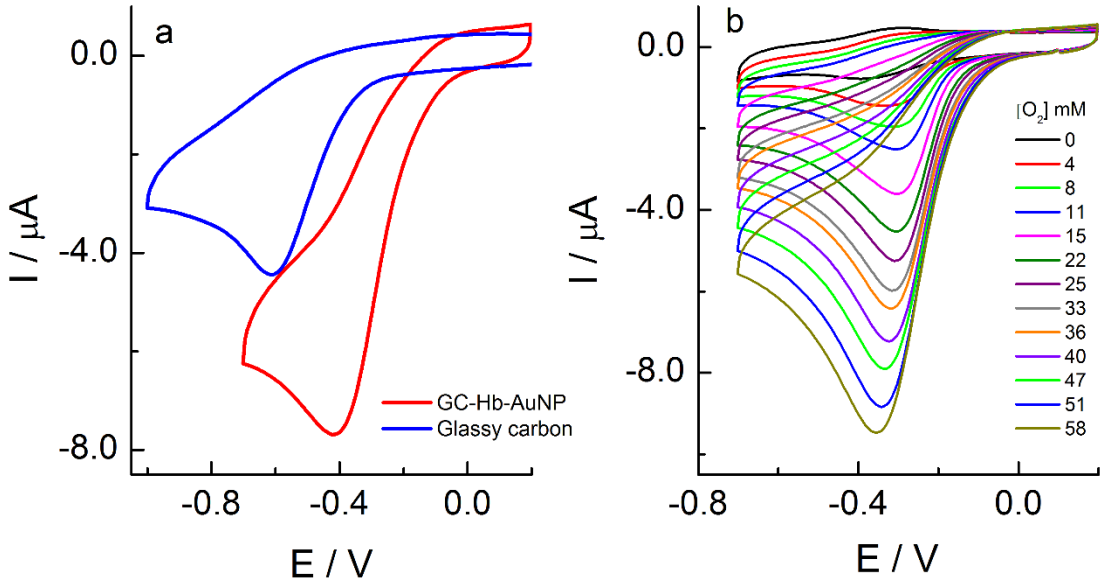

Figure 6. (a) Cyclic voltammogram for the reduction of O_2 (the concentration of O_2 is that of equilibrium). (b) Effect of the addition of increasing concentrations of O_2 to a 50 mM phosphate buffer solution at pH 7.4 with Hb-cAuNPs deposited on a glassy carbon electrode (O_2 has been added after elimination of the equilibrium concentration by bubbling N_2). Concentration of O_2 has been calculated by considering the volume of air added and an O_2 composition of 21%.

It is well known that Hb possesses oxygen carrying ability only in the ferrous state and binds O_2 giving place to the oxy-Hb species ($Fe(II)O_2$), while it loses this property when in the ferric form (Fe(III)), met-Hb. Under these conditions, we have examined the electrochemical behavior of the Hb-bioconjugates in the presence of O_2. As can be observed in Figure 6a, a reduction peak at -0.415 V is obtained in a phosphate buffer solution (pH 7) without removing the equilibrium O_2 concentration. For comparison, the voltammogram obtained with a naked GC electrode is also shown. The reduction peak for O_2 appears at -0.615 V, a potential 200 mV more negative than in the presence of the bioconjugate, indicating the electrocatalytic effect of the later.

In Figure 6b, the effect of increasing O_2 concentration is shown. After elimination of the O_2 present in the solution, the concentration was increased by introducing air by a syringe. As can be seen, the reduction peak current increases linearly with the concentration of O_2 in solution, and at the same time the oxidation peak of Hb disappears. The O_2 is reduced at the bioconjugate surface by the reaction [26, 47]:

$$2\ HbFe(II) + 4\ H^+ + O_2 + 2e \rightarrow 2\ HbFe(III) + 2\ H_2O$$

The electrocatalytic behavior of the bioconjugates in the reduction of H_2O_2 and O_2, can also be taken as a probe of the Hb maintaining its conformational stability upon interacting with the AuNPs. Moreover, the role of the later in the electrocatalytic activity is also demonstrated.

Conclusions

The immobilization of Hb around the protected c-, MP- and MUA-AuNPs gives place to bioconjugates that are stable in solution [16]. These bioconjugates are electroactive when deposited on a glassy carbon electrode whereas the free Hb is not active under the same experimental conditions. Hb exhibits a pair of well-defined quasi-reversible redox peaks in a wide pH range. Only the Hb molecules belonging to the first or second protein layers around the nanoparticle, exchange electrons efficiently pointing to an effect of the AuNP in the electron transfer process. The three AuNPs used in this study form bioconjugates that show similar electrochemical properties, indicating that the mode of binding on the AuNP surface does not affect the protein structural integrity. The Hb-AuNPs bioconjugates show good electrocatalysis to the reduction of hydrogen peroxide and oxygen indicating that such systems have potential applications in the construction of biosensors. Moreover, the role of the bioconjugates as a whole is of interest in our work that is focused on the behavior of AuNPs in living systems either for applications as nanosensors or in drug delivery systems.

Acknowledgements.

We thank the Ministerio de Economía y Competitividad (MINECO) (Projects CTQ2014-60227-R and CTQ-2015-71955-REDT Network of excellence Sensors and Biosensors), Junta de Andalucía (P10-FQM-6408) and University of Córdoba for financial support of this work.

References

[1] P. Vatsyayan, Recent Advances in the Study of Electrochemistry of Redox Proteins, in: F.-M. Matysik (Ed.) Trends in Bioelectroanalysis, Springer International Publishing, Cham, 2017, pp. 223-262.

[2] F.A. Armstrong, G.S. Wilson, Recent developments in faradaic bioelectrochemistry, Electrochim. Acta, 45 (2000) 2623-2645.

[3] F.A. Armstrong, Recent developments in dynamic electrochemical studies of adsorbed enzymes and their active sites, Current Opinion in Chemical Biology, 9 (2005) 110-117.

[4] L.H. Guo, H.A.O. Hill, Direct Electrochemistry of Proteins and Enzymes, Adv. Inorg. Chem., 36 (1991) 341-375.

[5] H.A.O. Hill, N.I. Hunt, Direct and Indirect Electrochemical Investigations of Metalloenzymes, Metallobiochemistry, Pt D, 227 (1993) 501-522.

[6] J. Yang, N.F. Hu, Direct electron transfer for hemoglobin in biomembrane-like dimyristoyl phosphatidylcholine films on pyrolytic graphite electrodes, Bioelectrochem. Bioenerg., 48 (1999) 117-127.
[7] H. Huang, N.F. Hu, Y.H. Zeng, G. Zhou, Electrochemistry and electrocatalysis with heme proteins in chitosan biopolymer films, Anal. Biochem., 308 (2002) 141-151.
[8] Q. Lu, C. Hu, R. Cui, S. Hu, Direct Electron Transfer of Hemoglobin Founded on Electron Tunneling of CTAB Monolayer, J. Phys. Chem. B, 111 (2007) 9808-9813.
[9] Y.X. Xua, C.G. Hu, S.S. Hu, A reagentless nitric oxide biosensor based on the direct electrochemistry of hemoglobin adsorbed on the gold colloids modified carbon paste electrode, Sensor Actuat. B-Chem., 148 (2010) 253-258.
[10] Y.L. Zhou, Z. Li, N.F. Hu, Y.H. Zeng, J.F. Rusling, Layer-by-layer assembly of ultrathin films of hemoglobin and clay nanoparticles with electrochemical and catalytic activity, Langmuir, 18 (2002) 8573-8579.
[11] K. Ariga, Q.M. Ji, T. Mori, M. Naito, Y. Yamauchi, H. Abe, J.P. Hill, Enzyme nanoarchitectonics: organization and device application, Chem. Soc. Rev., 42 (2013) 6322-6345.
[12] E.C. Dreaden, A.M. Alkilany, X. Huang, C.J. Murphy, M.A. El-Sayed, The golden age: gold nanoparticles for biomedicine, Chem. Soc. Rev., 41 (2012) 2740-2779.
[13] A.J. Viudez, R. Madueno, T. Pineda, M. Blazquez, Stabilization of gold nanoparticles by 6-mercaptopurine monolayers. Effects of the solvent properties, J. Phys. Chem. B, 110 (2006) 17840-17847.
[14] A.J. Viudez, R. Madueno, M. Blazquez, T. Pineda, Synthesis, Characterization, and Double Layer Capacitance Charging of Nanoclusters Protected by 6-Mercaptopurine, J. Phys. Chem. C, 113 (2009) 5186-5192.
[15] E. Reyes, R. Madueno, M. Blazquez, T. Pineda, Facile Exchange of Ligands on the 6-Mercaptopurine-Monolayer Protected Gold Clusters Surface, J. Phys. Chem. C, 114 (2010) 15955-15962.
[16] R. del Caño, L. Mateus, G. Sánchez-Obrero, J.M. Sevilla, R. Madueño, M. Blázquez, T. Pineda, Hemoglobin bioconjugates with surface-protected gold nanoparticles in aqueous media: The stability depends on solution pH and protein properties, J. Coll. Inter. Sci., 505 (2017) 1165-1171.
[17] T. Cedervall, I. Lynch, M. Foy, T. Berggad, S.C. Donnelly, G. Cagney, S. Linse, K.A. Dawson, Detailed identification of plasma proteins adsorbed on copolymer nanoparticles, Angew. Chem.-Int. Edit., 46 (2007) 5754-5756.
[18] M. Lundqvist, J. Stigler, G. Elia, I. Lynch, T. Cedervall, K.A. Dawson, Nanoparticle size and surface properties determine the protein corona with possible implications for biological impacts, Proc. Natl. Acad. Sci. U. S. A., 105 (2008) 14265-14270.

[19] M.P. Monopoli, F.B. Bombelli, K.A. Dawson, Nanobiotechnology. Nanoparticle coronas take shape, Nat. Nanotechnol., 6 (2011) 11-12.
[20] O. Vilanova, J.J. Mittag, P.M. Kelly, S. Milani, K.A. Dawson, J.O. Radler, G. Franzese, Understanding the Kinetics of Protein-Nanoparticle Corona Formation, Acs Nano, 10 (2016) 10842-10850.
[21] A. Salvati, A.S. Pitek, M.P. Monopoli, K. Prapainop, F.B. Bombelli, D.R. Hristov, P.M. Kelly, C. Aberg, E. Mahon, K.A. Dawson, Transferrin-functionalized nanoparticles lose their targeting capabilities when a biomolecule corona adsorbs on the surface, Nat. Nanotechnol., 8 (2013) 137-143.
[22] G. Brauer, Handbook of Preparative Inorganic Chemistry, Academic Press, New York, 1965.
[23] C.D. Keating, M.D. Musick, M.H. Keefe, M.J. Natan, Kinetics and thermodynamics of Au colloid monolayer self-assembly - Undergraduate experiments in surface and nanomaterials chemistry, J. Chem. Educ., 76 (1999) 949-955.
[24] S.H. Chen, R. Yuan, Y.Q. Chai, L.Y. Zhang, N. Wang, X.L. Li, Amperometric third-generation hydrogen peroxide biosensor based on the immobilization of hemoglobin on multiwall carbon nanotubes and gold colloidal nanoparticles, Biosens. Bioelectron., 22 (2007) 1268-1274.
[25] H.L. Guo, D.Y. Liu, X.D. Yu, X.H. Xia, Direct electrochemistry and electrocatalysis of hemoglobin on nanostructured gold colloid-silk fibroin modified glassy carbon electrode, Sensor Actuat. B-Chem., 139 (2009) 598-603.
[26] Y. Liu, T. Han, C. Chen, N. Bao, C.M. Yu, H.Y. Gu, A novel platform of hemoglobin on core-shell structurally Fe3O4@Au nanoparticles and its direct electrochemistry, Electrochim. Acta, 56 (2011) 3238-3247.
[27] J. Xuan, X.-d. Jia, L.-P. Jiang, E.S. Abdel-Halim, J.-J. Zhu, Gold nanoparticle-assembled capsules and their application as hydrogen peroxide biosensor based on hemoglobin, Bioelectrochemistry, 84 (2012) 32-37.
[28] L. Xie, Y. Xu, X. Cao, Hydrogen peroxide biosensor based on hemoglobin immobilized at graphene, flower-like zinc oxide, and gold nanoparticles nanocomposite modified glassy carbon electrode, Colloid Surf. B, 107 (2013) 245-250.
[29] F.P. Li, M.Z. Nie, X.L. He, J.J. Fei, Y.L. Ding, B. Feng, Direct electrochemistry and electrocatalysis of hemoglobin on a glassy carbon electrode modified with poly(ethylene glycol diglycidyl ether) and gold nanoparticles on a quaternized cellulose support. A sensor for hydrogen peroxide and nitric oxide, Microchim. Acta, 181 (2014) 1541-1549.
[30] L. Peng, S.Y. Dong, N. Li, G.C. Suo, T.L. Huang, Construction of a biocompatible system of hemoglobin based on AuNPs-carbon aerogel and ionic liquid for amperometric biosensor, Sensor Actuat. B-Chem., 210 (2015) 418-424.

[31] L.L. Zhang, G.Q. Han, Y. Liu, J. Tang, W.H. Tang, Immobilizing haemoglobin on gold/graphene-chitosan nanocomposite as efficient hydrogen peroxide biosensor, Sensor Actuat. B-Chem., 197 (2014) 164-171.

[32] H.O. Finklea, Electroanalytical Chemistry, Marcel Dekker, New York, 1996.

[33] E. Laviron, General expression of the linear potential sweep voltammogram in the case of diffusionless electrochemical systems, J. Electroanal. Chem., 101 (1979) 19-28.

[34] R.W. Murray, Electroanalytical Chemistry, Marcel Deckker, New York, 1984.

[35] M.F. Perutz, M.G. Rossmann, A.F. Cullis, H. Muirhead, G. Will, A.C.T. North, Structure of Haemoglobin-3-dimensional Fourier synthesis at 5.5-A resolution, obtained by X-ray analysis, Nature, 185 (1960) 416-422.

[36] A. Jimenez, A. Sarsa, M. Blazquez, T. Pineda, A Molecular Dynamics Study of the Surfactant Surface Density of Alkanethiol Self-Assembled Monolayers on Gold Nanoparticles as a Function of the Radius, J. Phys. Chem. C, 114 (2010) 21309-21314.

[37] J.J. Zhang, Y.G. Liu, L.P. Jiang, J.J. Zhu, Synthesis, characterizations of silica-coated gold nanorods and its applications in electroanalysis of hemoglobin, Electrochem. Commun., 10 (2008) 355-358.

[38] H.Y. Gu, A.M. Yu, H.Y. Chen, Direct electron transfer and characterization of hemoglobin immobilized on a Au colloid-cysteamine-modified gold electrode, J. Electroanal. Chem., 516 (2001) 119-126.

[39] A.J. Bard, L.R. Faulkner, Electrochemical Methods: Principles and Applications, 2ª ed., John Wiley and Sons, New York, 2001.

[40] G. Zhao, J.J. Feng, J.J. Xu, H.Y. Chen, Direct electrochemistry and electrocatalysis of heme proteins immobilized on self-assembled ZrO2 film, Electrochem. Commun., 7 (2005) 724-729.

[41] G. Zhao, J.J. Xu, H.Y. Chen, Fabrication, characterization of Fe3O4 multilayer film and its application in promoting direct electron transfer of hemoglobin, Electrochem. Commun., 8 (2006) 148-154.

[42] E. Topoglidis, C.J. Campbell, A.E.G. Cass, J.R. Durrant, Nitric oxide biosensors based on the immobilization of hemoglobin on mesoporous titania electrodes, Electroanalysis, 18 (2006) 882-887.

[43] X.J. Liu, W.J. Zhang, Y.X. Huang, G.X. Li, Enhanced electron-transfer reactivity of horseradish peroxidase in phosphatidylcholine films and its catalysis to nitric oxide, J. Biotechnol., 108 (2004) 145-152.

[44] Y.L. Zhou, N.F. Hu, Y.H. Zeng, J.F. Rusling, Heme protein-clay films: Direct electrochemistry and electrochemical catalysis, Langmuir, 18 (2002) 211-219.

[45] R.A. Kamin, G.S. Wilson, Rotating ring-disk enzyme electrode for biocatalysis kinetic studies and characterization of the immobilized enzyme layer, Anal. Chem., 52 (1980) 1198-1205.

[46] Y.Z. Xian, Y. Xian, L.H. Zhou, F.H. Wu, Y. Ling, L.T. Jin, Encapsulation hemoglobin in ordered mesoporous silicas: Influence factors for immobilization and bio electrochemistry, Electrochem. Commun., 9 (2007) 142-148.

[47] F.W. Scheller, N. Bistolas, S.Q. Liu, M. Janchen, M. Katterle, U. Wollenberger, Thirty years of haemoglobin electrochemistry, Adv. Colloid Interface Sci., 116 (2005) 111-120.

Graphical Abstract